Hindawi Publishing Corporation
Journal of Robotics
Volume 2010, Article ID 743010, 9 pages
doi:10.1155/2010/743010

Research Article

The New Evolution for SIA Rotorcraft UAV Project

Juntong Qi, Dalei Song, Lei Dai, Jianda Han, and Yuechao Wang

State Key Laboratory of Robotics, Shenyang Institute of Automation, CAS Nanta Street 114, Shenyang 110016, China

Correspondence should be addressed to Juntong Qi, qijt@sia.cn

Received 31 October 2009; Accepted 23 March 2010

Academic Editor: Zeng-Guang Hou

This paper describes recent research on the design, implement, and testing of a new small-scaled rotorcraft Unmanned Aerial Vehicle (RUAV) system—ServoHeli-40. A turbine-powered UAV weighted less than 15 kg was designed, and its major components were tested at the Shenyang Institute of Automation, Chinese Academy of Sciences in Shenyang, China. The aircraft was designed to reach a top speed of more than 20 mps, flying a distance of more than 10 kilometers, and it is going to be used as a test-bed for experimentally evaluating advanced control methodologies dedicated on improving the maneuverability, reliability, as well as autonomy of RUAV. Sensors and controller are all onboard. The full system has been tested successfully in the autonomous mode using the multichannel active modeling controller. The results show that in a real windy environment the rotorcraft UAV can follow the trajectory which was assigned by the ground control station exactly, and the new control method is obviously more effective than the one in the past year's research.

1. Introduction

Unmanned aerial vehicles (UAVs) are useful for many applications where human intervention is considered difficult or dangerous. Traditionally, the fixed-wing UAV has been served as the unit for these dangerous tasks because the control is easy. Rotary-wing UAV, on the other hand, can be used in many different tasks where the fixed-wing one is unable to achieve, such as vertical take-off/landing, hovering, lateral flight, pirouette, and bank-to-turn. Due to the versatility in maneuverability, helicopters are capable to fly in and out of restricted areas and hover efficiently for long periods of time. These characteristics make RUAV applicable for many military and civil applications.

However, the control of RUAV is difficult. Although some control algorithms have been proposed [1–6], most of them were verified by simulation instead of real experiments. One reason for this is due to the complicate, nonlinear, and inherently unstable dynamics, which has cross coupling between main and tail rotor, and lots of time-varying aerodynamic parameters. Another reason is that the flight test is in high risk. If an RUAV lost its control, it would never be stabilized again.

Based on our UAV research in [7], this paper details the development of a new unmanned helicopter (UAV) test bed—ServoHeli-40 (Figure 1) and the advanced control experiments performed toward achieving full autonomous flight. The experimental platform which has 40 kilograms takeoff weight is designed and finished by our research group in Shenyang Institute of Automation, Chinese Academy of Sciences. The brief of this paper is as follows: the ServoHeli-40 platform is introduced in Section 2. The introduction of sensor package is in Section 3. The modeling of the UAV helicopter system is presented in Section 4. In Section 5, we introduce active modeling scheme as a baseline control of the platform. In the end, there will be a conclusion of our work and also some discussions about future research issues.

2. ServoHeli-40 Platform Description

The entire experiment was implemented on the ServoHeli-40 small-size helicopter platform (Figure 1).

ServoHeli-40 aerial vehicle is a high-quality helicopter, which is changed by us using an RC technical grade helicopter operating with a remote controller. The modified

Figure 1: ServoHeli-40 small-size helicopter platform.

Table 1: Physical characteristics of ServoHeli-40 small-size helicopter.

Length	2.12 m
Height	0.73 m
Main rotor diameter	2.15 m
Stabilizer bar diameter	0.75 m
Rotor speed	1450 rpm
Dry weight	20 kg
Engine	2-stroke, air cooled
Flight time	45 min

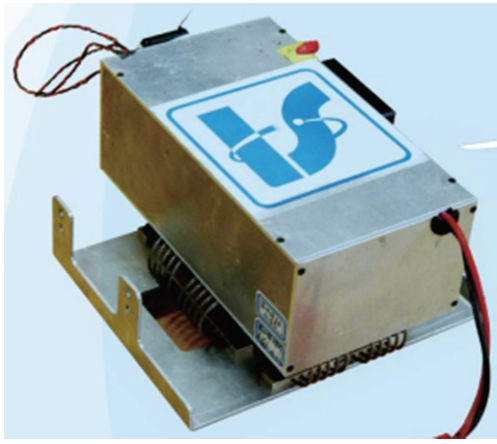

Figure 2: Airborne control box.

Figure 4: Hemisphere OEM GPS.

Figure 3: Crossbow IMU.

Figure 5: HMR3000 digital compass.

system allows a payload of more than 10 kilograms, which is sufficient to take the whole airborne avionics box and the communication units for flight control. The fuselage of the helicopter is constructed with sturdy duralumin, and composite body and the main rotor blades are replaced with heavy-duty fiber glass reinforced ones to accommodate extra payloads. The vehicle is powered by a ZENOAH engine which generates 9 hp at about 10000 rpm, a displacement of 80 cc, and practical angular rate ranging from 2,000 to 16,000 rpm. The full length of the fuselage is 2120 mm as well as the full width of it is 320 mm. The total height of the helicopter is 730 mm, the main rotor is 2150 mm, and the tail rotor is 600 mm.

Designing the avionics box and packing the box appropriately under the fuselage of the helicopter are two main tasks to implement of this UAV helicopter system. In the actual flight environment, the weight and the size of the avionics box are strict limited. Our airborne control box, which is shown in Figure 2, is a compact aluminum alloy package mounted on the landing gear. The center of gravity of the box lies on the IMU device, where it is not the geometry center of the system that keeps the navigation data

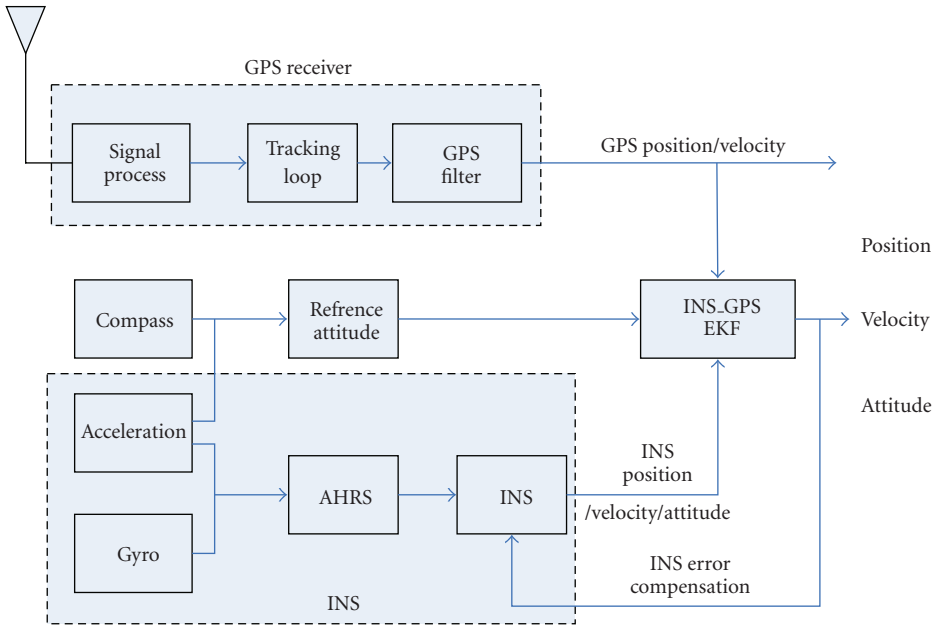

Figure 6: GPS-INS Navigator Structure.

from IMU accurate. The compass and the IMU are taken as the horizontal center of the gravity of the avionics system and the other components are installed on the same line.

The platform, which is fixed with a 3-axis gyro, a three-axis acceleration sensor, a compass, and a GPS, can save the data of velocities, angular rates, Euler angle accelerations, and positions into an SD card through an ARM processor. An Extended Kalman Fliter is used to estimate the sensors values. There is a CPLD used for sampling control inputs from the remote control of the pilot. The rotor speed is controlled by a Governor, an electronic unit for engine control. Table 1 shows the physical characteristics of ServoHeli-40 small-size helicopter. The type of the sensors and the method for navigation will be described in the next section.

3. Sensors of the ServoHeli-40

3.1. Sensors for Attitude and Position Estimation. In order to navigate following a desired trajectory while stabilizing the vehicle, the information about helicopter position, velocity, acceleration, attitude, and the angular rates should be known to the guidance and control system. The rotorcraft UAV system is equipped with sensors including inertial sensor unit, GPS, digital compass, rotor speed sensor, air-press altimeter, and ultrasonic sensor to obtain above accurate information about the motion of the helicopter in association with environmental information.

The Crossbow IMU300, which is shown in Figure 3, is a six-axis measurement system designed to measure the linear acceleration along three orthogonal axes and rotation rate around three orthogonal axes. It employs on-board digital processing to provide application-specific outputs and to compensate for deterministic error sources within the unit. Solid-state MEMS sensors make the IMU300 product responsive and reliable.

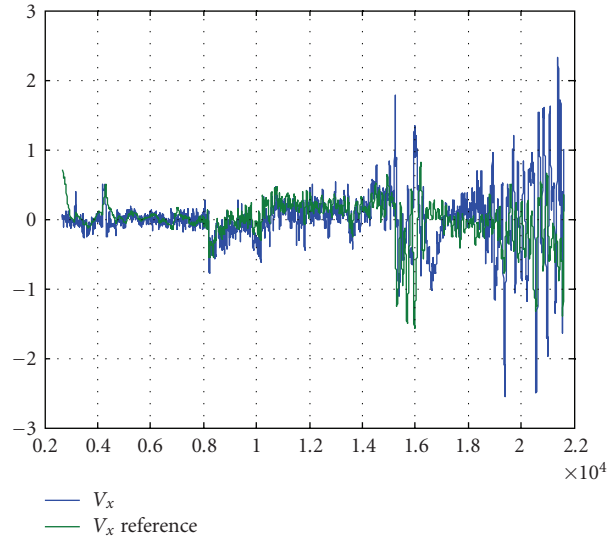

Figure 7: Velocities before and after filtering.

Hemisphere GPS, which is shown in Figure 4, is a space-based satellite radio navigation system developed by a Canada company. GPS provides three-dimensional position and time with the deduced estimates of velocity and heading. The GPS provides position estimates at up to 10 Hz. For operation, the GPS and the antenna are installed on the host aerial vehicle.

HMR3000 digital compass, which is presented in Figure 5, is an electronic compass module that provides yaw, pitch, and roll output for navigation and guidance systems. This compass provides fast refrash rate of up to 20 Hz and a high accuracy of 0.5 degree with 0.1-degree resolution.

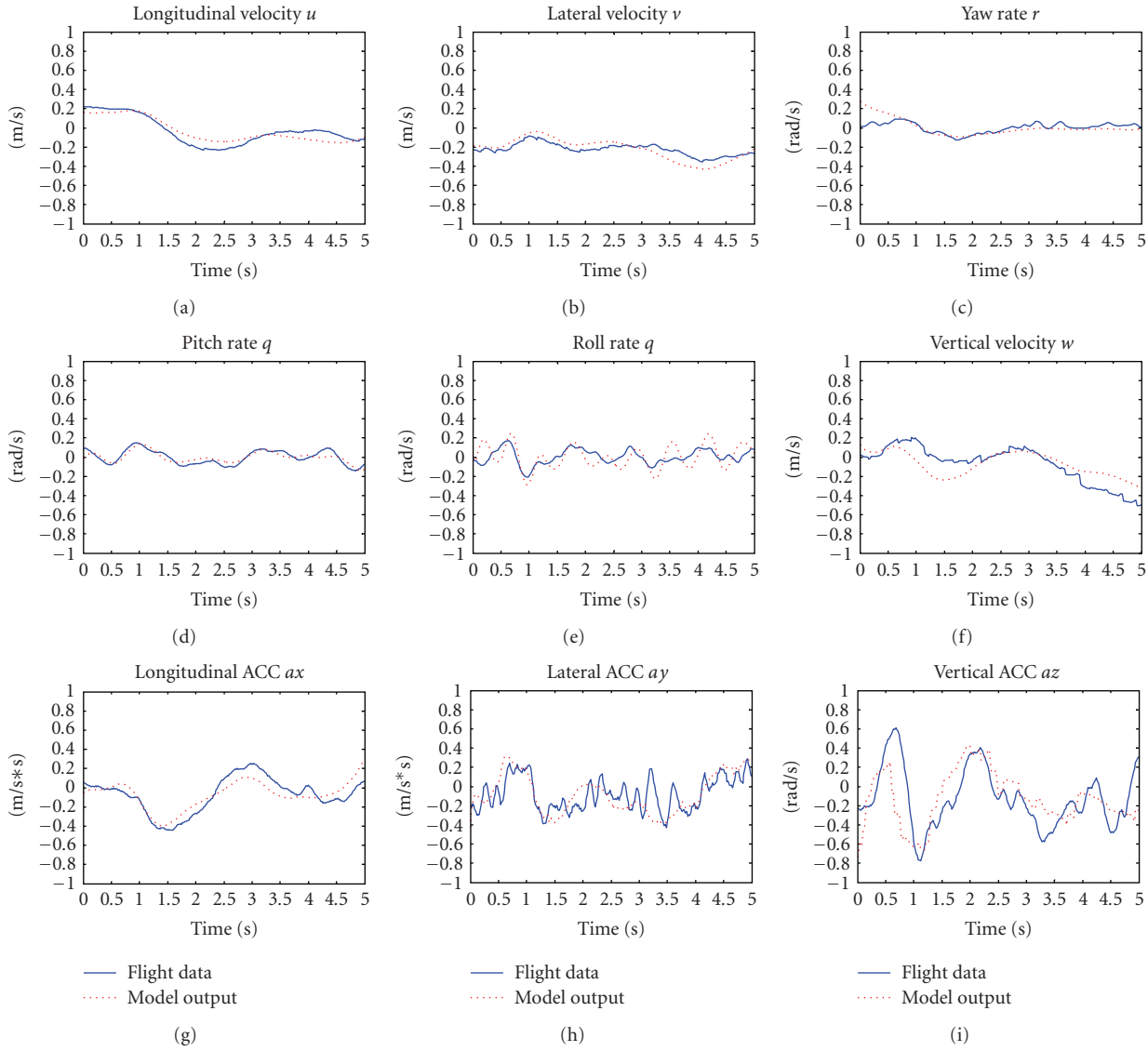

Figure 8: Rotorcraft UAV modeling verification.

In order to get the accurate altitude information of the vehicle, an air-pressure altimeter that is collecting data higher than 5 meters as well as an ultrasonic sensor that is getting the information on other situations is equipped under the avionics box.

The update rate of all sensors is ranging from 10 to 100 Hz, which is enough for implementation for advanced control algorithms.

3.2. EKF Based Navigator Design. In our avionics box, we use rate gyros and accelerometers to measure rates about three axes and accelerations along 3 axes; an independent ARM processor is used to extract absolute roll and pitch. However, in the real flight environment, the sensors will be subjected to rotor frequency vibrations; both the rate and acceleration readings are grossly inaccurate and consequential; so it is the attitude estimation.

In order to isolate the unit from these frequencies, we use EKF method to build an effective navigator for flight information estimation. The proposed GPS_INS Navigator is in Figure 6, and a typical plot of the forward velocities before and after filtering is given in Figure 7.

4. Rotorcraft UAV Modeling

For effective hovering identification, the original model in [8] is decomposed into three groups (longitudinal, lateral, and yaw-heave coupling), and a semidecoupled model is obtained. Each group has a decoupled system matrix, and the coupling characteristics are presented only in the control matrix. Thus, the number of unknown parameters and control inputs is reduced and the control loops are semidecoupled. Then, to identify the unknown parameters in the MIMO semidecoupled model, a new cost function is

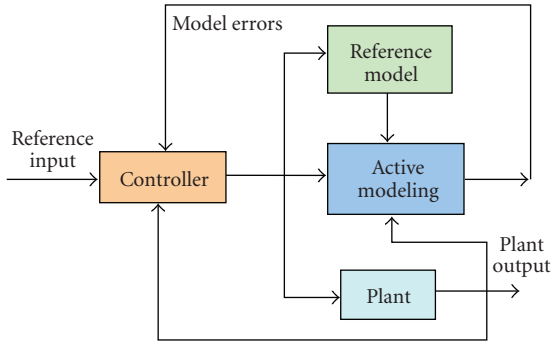

Figure 9: The scheme of active model-based control.

Figure 10: ServoHeli-40 small-size helicopter platform for experiment use.

proposed to make the traditional method of SISO system frequency estimation [9] applicable to the MIMO state-space models. The proposed cost function is presented in the addition form of the frequency error of every input-output pair for transfer matrix, and the parameters are identified by minimizing the cost function. The simplified model and proposed identification method free the selection of initial estimation and constraint is not required.

We have got the numerical model, and then the other serial of input data was tested using the proposed model. The blue line is the measurement of the yaw rate from the real flight as well as the red line is calculated by the numerical model and the real flight input. As is shown in Figure 8, the estimation output is similar to the real flight data and we can conclude that the proposed modeling method is useful to the rotorcraft UAV.

5. Active Modeling Control Scheme

Figure 9 illustrates the active model-based control scheme. The error between the reference model and the actual dynamics of the controlled plant is estimated by an online modeling strategy. The control, which is designed according to the reference model, should be able to compensate the estimated model error and fix it in real time. In the followings of this paper, we use the Adaptive Set Membership Filter (ASMF) [10] as the active modeling algorithm and the modified GPC as the control.

For normal missions of an unmanned helicopter, the flight modes include hovering (velocity under 5 m/s), cruising (velocity above 5 m/s), taking off and landing (distance to the ground is below 3 m while significant ground effect exists), and the transitions among these modes. A reference model is typically obtained by linearizing the nonlinear dynamics of a helicopter at one flying mode. The model errors from linearization, external disturbance, simplification, and unmodeled dynamics can be considered as additional process noise. Thus, a linearized state-space model for helicopter dynamics in full flight envelope can be formulated as

$$\begin{aligned} \dot{X} &= A_0 X + B_0 U + B_f f(X, \dot{X}, W), \\ Y &= CX, \end{aligned} \tag{1}$$

where $X \in R^{13}$ is the state, including 3-axis velocity, pitch and roll angle, 3-axis gyro values, flapping angles of main rotor and stabilizer bar, and the feedback of yaw gyro. $Y \in R^8$ is the output, including 3-axis velocity, pitch and roll angle, and 3-axis gyro values, A_0 and B_0 contain parameters that can be identified in different flight modes, and we use them to describe the parameters in hovering mode. $U \in R^4$ is the control input vector. The detail of building the nominal model and physical meaning of parameters is explanted in [11].

To describe the dynamics change, in (1), here, we introduce $f(X, \dot{X}, W, t) \in R^{13}$ to represent the time varying model error in full flight envelope, and $W \in R^{13}$ is the process noise.

5.1. Velocity Tracking Control. All flight tests are performed on the ServoHeli-40 setup (Figure 10), which was developed in the State Key Laboratory, SIACAS. It is equipped with a 3-axis gyro, a 3-axis accelerometer, a compass, and a GPS. The sensory data can be sampled and stored into an SD card through an onboard DSP.

Generalized predictive control (GPC), stationary increment predictive control (SIPC), and active model-based stationary increment predictive control (AMSIPC), which are proposed by us in [11], were all tested in the same flight conditions, and the comparison results are shown in Figures 11–13. The identified parameters were in [12] as nominal model.

It can be seen that when the helicopter increases its longitudinal velocity and changes flight mode from hovering to cruising, GPC (brown line) has a steady velocity error and increasing position error because of the model errors. SIPC (blue line) has a smaller velocity error because it uses increment model to reject the influence of the changing operation point and dynamics' slow change during the flight. However, the increment model may enlarge the model errors due to the uncertain parameters and sensor/process noises, resulting in the oscillations in the constant velocity period (clearly seen in Figures 11 and 12). While for AMSIPC (green line), because the model error has been online estimated

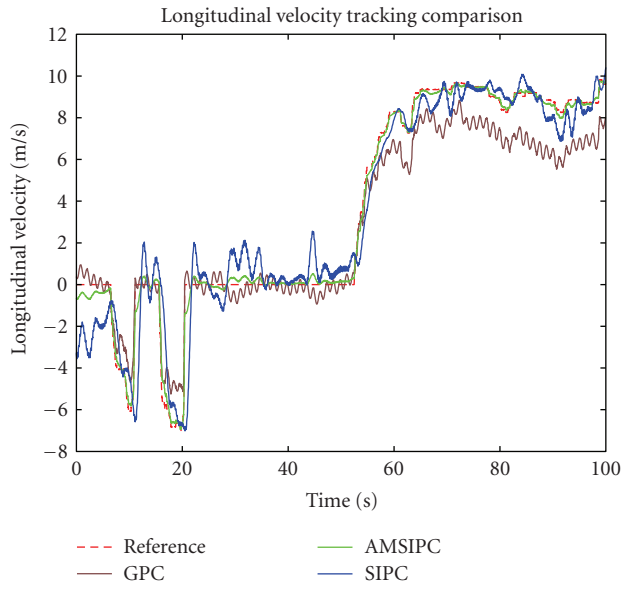

Figure 11: Longitudinal tracking results.

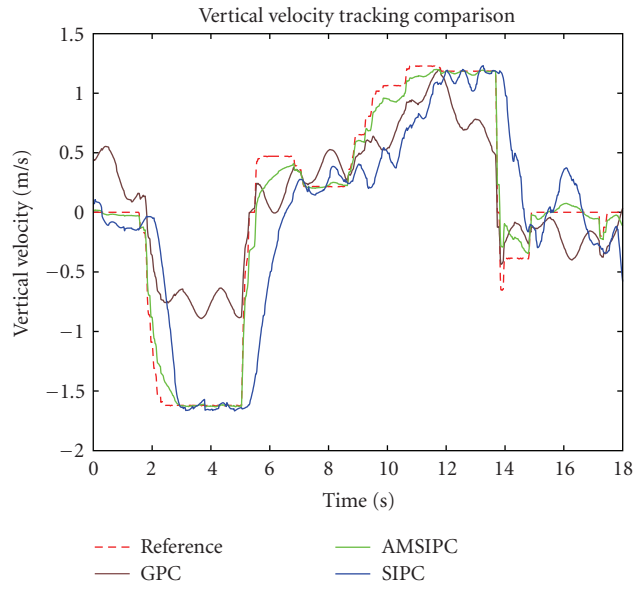

Figure 13: Vertical tracking results.

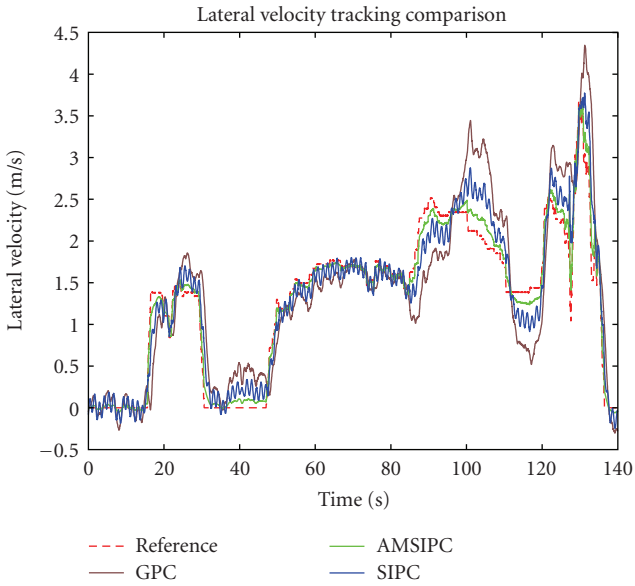

Figure 12: Lateral tracking results.

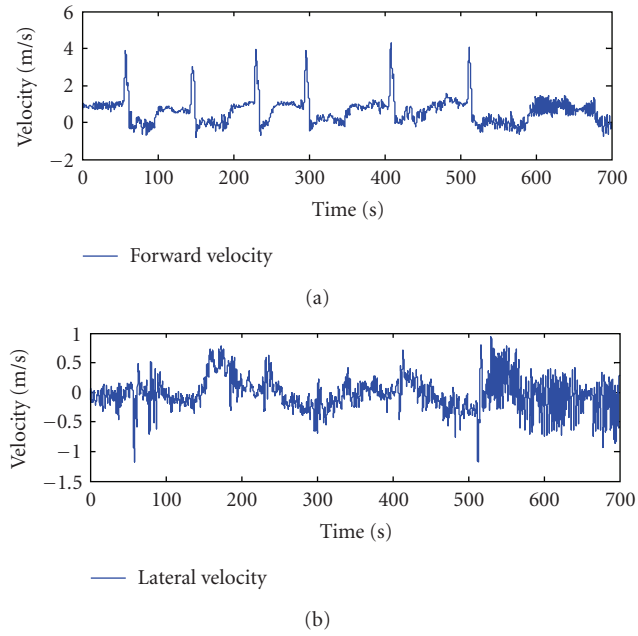

Figure 14: Forward and lateral velocity during the flight.

by the ASMF, the proposed AMSIPC successfully reduces velocity oscillations and tracking errors.

5.2. Preliminary Autonomous Flight Result. A two-loop control scheme for the rotorcraft UAV system was designed and tested using the ServoHeli-40 platform, in [7]. Some specified trajectories were designed to be flown. These trajectories were selected in order to evaluate the inner loop and outer loop response over several different sequences of inputs. We selected a tunnel way to be followed, as is shown in Figure 16. The proposed controller handled this flight trajectory with minimal error; see Figure 17. Figures 14 and 15 show that the angles and velocities which are controlled by inner loops also get a stable response.

5.3. New Flight Result. In this experiment, the identified hovering model was selected as nominal model for PID controller parameters calculation. The helicopter flies between two selected points, point A and point B. In the flight, the helicopter turns head 180° to point B at point A first; then, the helicopter increases the longitudinal velocity from 0 m/s to 10 m/s. When the helicopter arrives at point B, it decreases the longitudinal velocity from 10 m/s to 0 m/s and flies back to point A in the same way. To verify the strategy for estimate

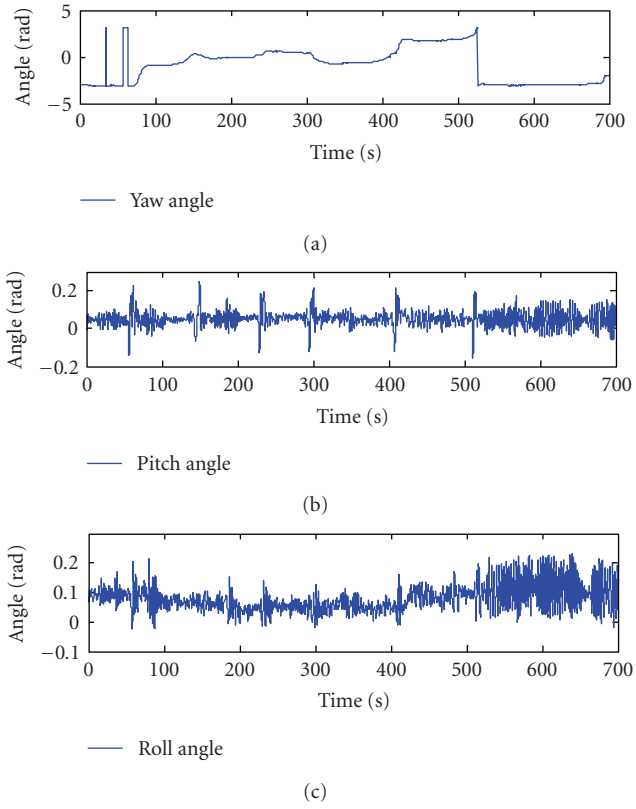

Figure 15: 3-axes angles during the flight.

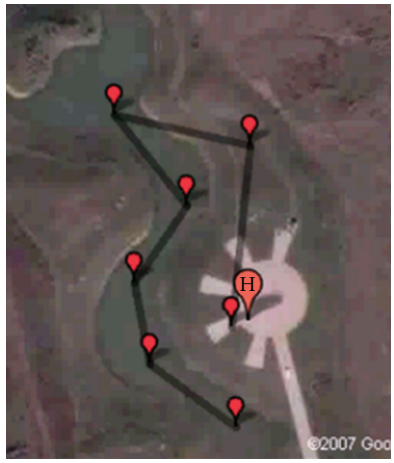

Figure 16: Trajectory in the Google Map.

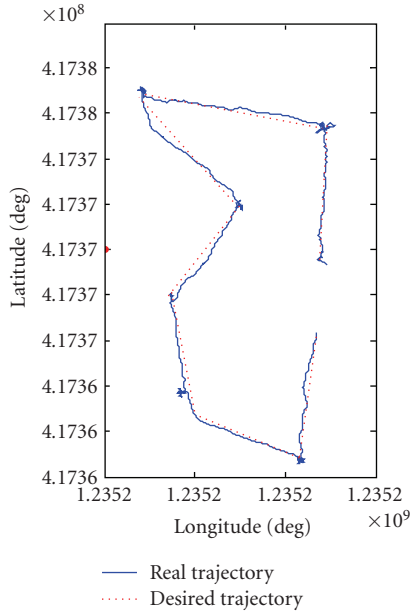

Figure 17: Desired and real trajectory.

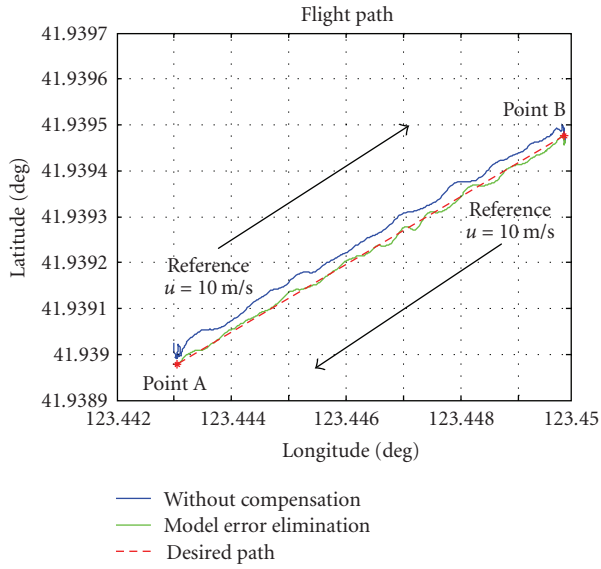

Figure 18: Flight path for test.

and elimination of the online model error, during the flight, we only use the PI controller without the strategy of model error elimination before time 150 seconds and compensate for the model error after that time in order to show the necessity of the strategy for model-error estimation and elimination. The flight path and position tracking errors are shown in Figures 18-19, and Figure 20 shows longitudinal velocity in the flight experiment. The wind in the flight environment is 3–6 m/s from the southeast.

It is clearly seen in Figures 18–20 that when the helicopter increases the longitudinal velocity and changes flight mode from hovering to cruise, the adaptive set-membership filter estimates the nonzero model errors and the estimated model error boundaries converge into the constant ellipse intersection, which means that the filter is stable. The effect of the strategy can be clearly seen in Figures 18–20, the lateral and vertical position errors decrease into 0.5 m, and the accuracy of longitudinal velocity tracking increases after the compensation, while nominal PID controller cannot get rid of the wind disturbance and changing flight mode that cause position error.

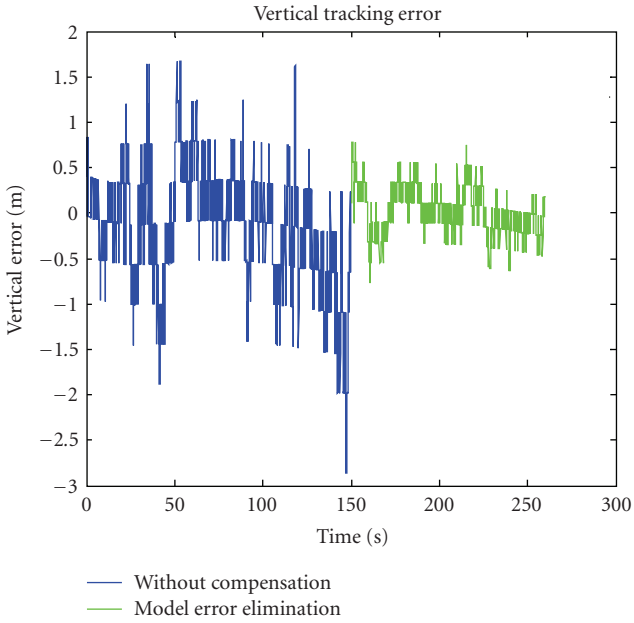

Figure 19: Vertical tracking error in real flight.

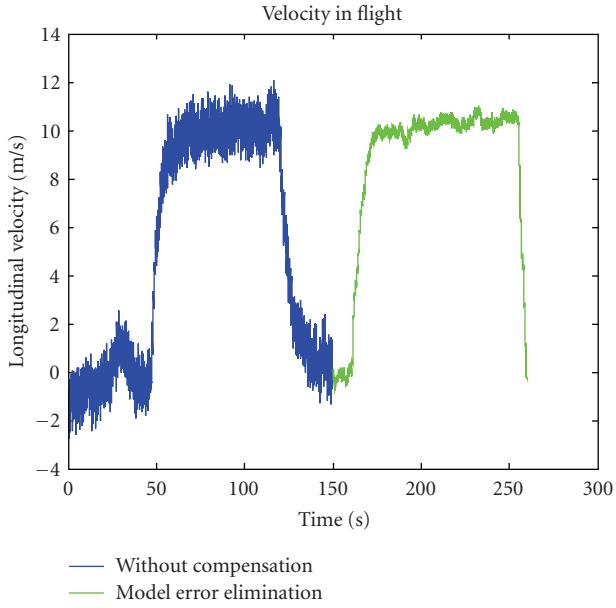

Figure 20: Longitudinal velocity in the flight.

6. Conclusions

This paper describes the current status of the ServoHeli-40 autonomous helicopter. We have introduced the system implementation of the rotorcraft UAV and control scheme for model-scaled helicopter. A reliable helicopter is built as the basic helicopter, which is changed to adapt to a heavier load in the future. We also introduce the sensors and algorithm for attitude and position estimation. The active modeling control and navigator works better than the two loop linear control scheme, which is applied by us in [7] last year.

The rotorcraft UAV system has been tested successfully for full autonomous flight including autonomous taking off and landing. The next step is to integrate the visual and IMU estimation into a unified sensor suite and to develop advantage autonomous flight control algorithm for maneuverable fight.

Acknowledgments

This work was supported by a Grant from the National High Technology Research and Development Program of China (863 Program) (no. 2007AA041503). The authors gratefully acknowledge the contribution of Shenyang Institute of Automation, Chinese Academy of Sciences, and reviewers' comments.

References

[1] C. P. Sanders, P. A. DeBitetto, and E. Feron, "Hierarchical control of small autonomous helicopters," in *Proceedings of the 37th IEEE Conference on Decision & Control*, vol. 4, pp. 3629–3634, Tampa, Fla, USA, December, 1998.

[2] M. A. Garratt and J. S. Chahl, "Visual control of an autonomous helicopter," in *Proceedings of the 41st Aerospace Sciences Meeting and Exhibit*, Reno, Nev, USA, January 2003.

[3] R. Enns and J. Si, "Helicopter ight control design using a learning control approach," in *Proceedings of the 39th IEEE Conference on Decision and Control*, pp. 1754–1759, Sydney, Australia, 2000.

[4] B. Bijnens, Q. P. Chu, G. M. Voorsluijs, and J. A. Mulder, "Adaptive feedback linearization flight control for a helicopter UAV," in *Proceedings of the AIAA Guidance, Navigation, and Control Conference and Exhibit*, vol. 6, pp. 4463–4472, San Francisco, Calif, USA, August 2005.

[5] T. J. Koo, D. H. Shim, O. Shakernia, et al., "Hierarchical hybrid system design on Berkeley UAV," in *Proceedings of the International Aerial Robotics Competition (IARC '98)*, Richland, Wash, USA, August 1998.

[6] Z. Jiang, J. Han, Y. Wang, and Q. Song, "Enhanced LQR control for unmanned helicopter in hover," in *Proceedings of the 1st International Symposium on Systems and Control in Aerospace and Astronautics*, pp. 1438–1443, Harbin, China, January 2006.

[7] J. Qi, D. Song, L. Dai, and J. Han, "The ServoHeli-20 rotorcraft UAV project," in *Proceedings of the 15th International Conference on Mechatronics and Machine Vision in Practice (M2VIP '08)*, pp. 92–96, Auckland, New Zealand, December 2008.

[8] B. Mettler, C. Dever, and E. Feron, "Scaling effects and dynamic characteristics of miniature rotorcraft," *Journal of Guidance, Control, and Dynamics*, vol. 27, no. 3, pp. 466–478, 2004.

[9] J. S. Bendat and A. G. Piersol, *Engineering Application of Correlation and Spectral Analysis*, John Wiley & Sons, New York, NY, USA, 1993.

[10] B. Zhou, J. Han, and G. Liu, "A UD factorization-based nonlinear adaptive set-membership filter for ellipsoidal estimation," *International Journal of Robust and Nonlinear Control*, vol. 18, no. 16, pp. 1513–1531, 2008.

[11] D. Song, J. Qi, and J. Han, "Active modeling based model predictive control for yaw-heave coupling dynamics of unmanned helicopters in full flight envelope," in *Proceedings of the AUVSI's Unmanned Systems North America*, vol. 1, pp. 108–121, 2009.

[12] D. L. Song, J. T. Qi, L. Dai, J. D. Han, and G. L. Liu, "Modeling a small-size unmanned helicopter using optimal estimation in the frequency domain," *International Journal of Intelligent Systems Technologies and Applications*, vol. 8, pp. 70–85, 2010.